Available online at www.sciencedirect.com
SCIENCE DIRECT
Earth and Planetary Science Letters 241 (2006) 863–875
EPSL
www.elsevier.com/locate/epsl

Late glacial to Holocene paleoenvironmental evolution of the Black Sea, reconstructed with stable oxygen isotope records obtained on ostracod shells

André Bahr [a,*], Helge W. Arz [b], Frank Lamy [b], Gerold Wefer [a]

[a] Universität Bremen, Fachbereich 5-Geowissenschaften, Postfach 33 04 40, D-28334 Bremen, Germany
[b] GeoForschungsZentrum Potsdam, Section 3.3, Telegrafenberg, D-14473 Potsdam, Germany

Received 22 April 2005; received in revised form 14 October 2005; accepted 27 October 2005
Available online 5 December 2005
Editor: H. Elderfield

Abstract

High-resolution stable oxygen isotope ($\delta^{18}O$ on ostracod shells), XRF-scanning and bulk grain-size data obtained on a transect of 6 gravity cores from the continental slope in the northwestern Black Sea give new insight into the hydrological evolution of the Black Sea since the Last Glacial Maximum (LGM). Stable climatic conditions during the LGM were followed by a series of meltwater pulses between 18 and 15.5 kyr BP that resulted in temporary isotopic depletion of the Black Sea waters. Subsequently, steadily increasing $\delta^{18}O$ values in all cores are mainly caused by isotopically enriched precipitation at the onset of the Allerød/Bølling warm period. A comparison of the major trends in $\delta^{18}O$ at different water depths suggests evaporation-driven deep water formation since ~14.5 kyr BP, while the two shallowest cores from 168 and 465 m water depth were under the influence of increased warming in the upper water column since 14.5 and 12.5 kyr BP, respectively. The core from 168 m depth seems to be additionally influenced by freshwater input of the Danube. This core provides a high-resolution record from the Younger Dryas/Allerød boundary and suggests that a NAO-like climate mode was governing the interannual variability in the run-off of the Danube, which implies that this climate mode has been a persistent climatic feature over central Europe. The inflow of saline Mediterranean waters occurs between 9 and 8 kyr BP, where a merging of all $\delta^{18}O$ records signals an initial homogenisation of the water column.

Keywords: Black Sea; paleohydrology; late glacial; oxygen isotopes; ostracods; NAO

1. Introduction

The late glacial and Holocene evolution of the Black Sea–Marmara Sea area received increasing scientific and public attention during the past decades, especially after Ryan and Pitman [1] published their theory of a catastrophic flooding of the Black Sea shelf through inflowing Mediterranean waters ca. 7500 yr ago (later corrected to 9.4 kyr BP [2]; ages calibrated to calendar years), also known as "Noah's Flood hypothesis". In order to test this hypothesis, numerous researchers tried to reconstruct the hydrologic evolution of the Black Sea. Hydraulic modeling studies [3,4] added some skepticism concerning the physical plausibility of such a flood. Myers et al. [3] do however not exclude

* Corresponding author. Tel.: +49 421 218 65670; fax: +49 421 218 65505.
E-mail address: bahr@uni-bremen.de (A. Bahr).

0012-821X/$ - see front matter © 2005 Elsevier B.V. All rights reserved.
doi:10.1016/j.epsl.2005.10.036

the possibility of a (in geologic terms) fast filling of the Black Sea within a few decades and Sidall et al. [5] stated that the morphological features for a very rapid inflow of Mediterranean water as expected from their model could indeed be found on the sea-floor near the Bosphorus entrance into the Black Sea. Paleoenvironmental reconstructions using pollen analysis [6], seismic stratigraphy [7], as well as foraminiferal and isotopic indicators [8] raised serious doubts about a catastrophic flooding of the Black Sea, while the finding of submerged shorelines at −155 m water depth [9] and salinity-reconstructions from the Sea of Marmara [10] seem to support the theory.

Stable oxygen isotope records from the Black Sea itself could give valuable insight into the salinification history. However, rather few records are presently available [2,11,12], and most of them reveal a rather low time resolution. The main reason is that stable isotope studies in the Black Sea are hampered by the scarcity of appropriate biogenic material and dating uncertainties because of unknown reservoir effects for the pre-marine sediments. For the present study, we obtained $\delta^{18}O$ records on ostracod shells on different cores from a NW Black Sea outer shelf to slope transect (168–1977 m water depth) that provide information about the development of the Black Sea water column between 28.5 and 8 kyr BP.

In addition to the Holocene connection with the Sea of Marmara, the Black Sea experienced a period of connection to the Caspian Sea, when meltwater from Scandinavian ice sheets rose the water level of the Caspian Sea over the height of the Manych depression [2,13,14]. This period is documented in the Black Sea by the deposition of a series of reddish-brown clay layers [12,15], roughly contemporaneous to Heinrich Event 1, when major parts of the Laurentide and other Northern Hemisphere ice sheets started to collapse [16]. To evaluate the sensitivity of the Black Sea towards such freshwater inflow is another important subject of this study.

The oxygen isotopic composition of lake water depends on several factors such as the isotopic composition of precipitation ($\delta^{18}O_{prec}$) and runoff ($\delta^{18}O_{run\text{-}off}$) entering the lake as well as the isotopic composition of the evaporated water, which again is dependent on factors like relative humidity, temperature and the $\delta^{18}O$ of atmospheric water vapour above the lake surface. Quantification of these parameters for the pre-Holocene Black Sea is hardly possible because the present hydrology of the Black Sea basin is considerably different from its pre-Holocene state: today the Black Sea has a connection to the Mediterranean Sea via the Sea of Marmara and shows a stable two-layer stratification with permanent anoxia in the deep basin [17], while the ancient Black Sea is generally thought to have been a freshwater lake, disconnected from the open ocean without permanent anoxia. Although quantitative estimations might be difficult to assess, stable oxygen isotopes provide useful qualitative insights into the changes the Black Sea underwent during the last ca. 30,000 yr.

2. Study area

The study area is situated in the NW Black Sea south of the Danube delta (Fig. 1) and comprises a transect of gravity cores from the outer shelf in 118 m water depth down to 1977 m on the lowermost slope (Table 1). The NW Black Sea shelf includes almost 94% of the total shelf area in the Black Sea [18]. The continental slope is very gentle and shaped by the morphology of the pre-Holocene Danube delta fan, which reaches far out towards the centre of the western Black Sea basin. Although the Danube transports 51.7 million tons per year (multi-annual mean [19]) of sediments to the NW Black Sea, the outer shelf is covered only by a very thin blanket of Holocene sediments and in some parts the Holocene is completely absent. This is caused by the strong (>50 cm s^{-1}) cyclonic "Rim Current" [20], which transports most of the suspended sediments alongside the coast to the south [18] (Fig. 1).

The western Black Sea is influenced by three different climate regimes: first by the humid conditions of SE Europe with an annual precipitation > 1000 mm yr^{-1}; second by the more continental climate in the northern part of the Black Sea and the eastern Danube lowlands with <600 mm yr^{-1} rainfall and, third, by the Mediterranean climate regime with winter rainfall in the south towards the Sea of Marmara [6]. Today the Black Sea has a positive water balance, i.e., the input by freshwater sources (300 km^3 yr^{-1} precipitation; 350 km^3 yr^{-1} runoff waters) exceeds the loss by evaporation (350 km^3 yr^{-1}); the net-difference in the freshwater budget is compensated by the net flux through the Bosphorus [17]. The hydrography of the Black Sea is characterised by a stable pycnocline between 100 and 200 m water depth that separates less saline near-surface water (18‰ salinity) from the more saline (22.5‰) deep water of Mediterranean origin. Since there is almost no exchange between both water masses, anoxia prevails below ca. 150 m, although the oxic/anoxic boundary can shift tens of meters in a few years [21].

$\delta^{18}O$-values of Black Sea waters mirror the present hydrological state: they vary around −2.8‰ in the

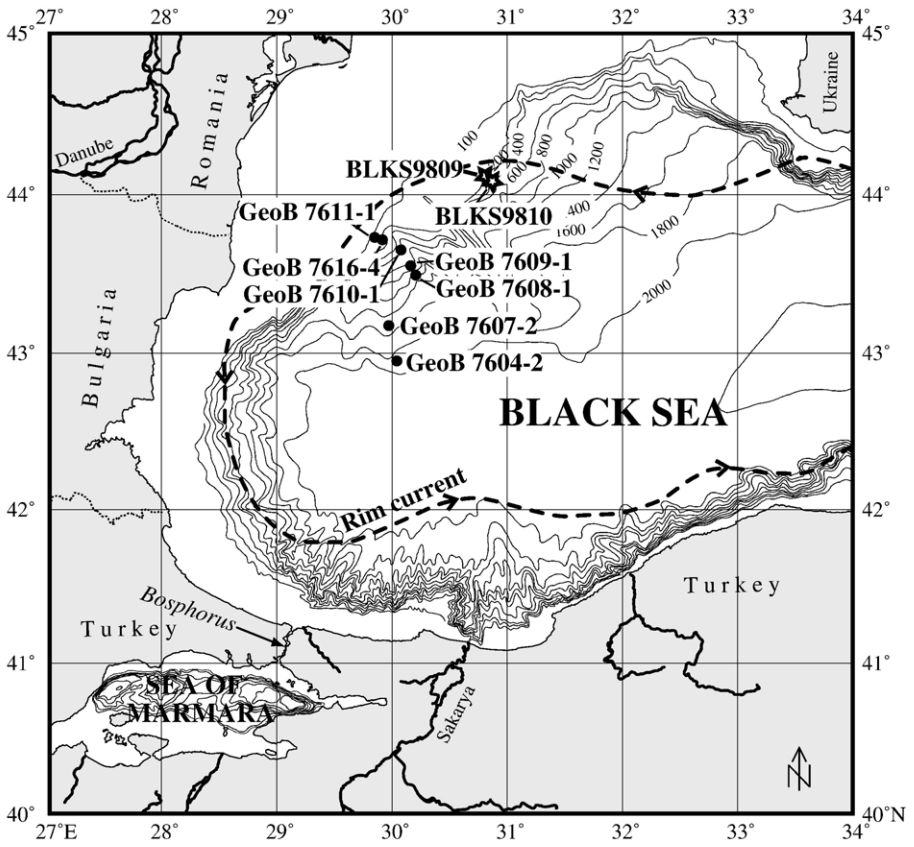

Fig. 1. Location of gravity cores recovered during *RV Meteor* cruise M51-4 in December 2001 (circles) and location of the two cores presented in Major et al. [12] (stars). Also indicated is the approximate position of the present Black Sea rim current [7].

upper 50 m and −1.8‰ in depths>500 m [22]. The area of investigation is substantially influenced by the freshwater input of the Danube with a multiannual mean water discharge of 190.7 km^3 yr^{-1} (before damming of the river [18]), which accounts for more than 50% [17] of the total river-runoff flowing into the Black Sea. The freshwater influence leads to considerably depleted $\delta^{18}O$ values of −10.5‰ near the Danube river mouth and −3‰ on the NW Black Sea shelf close to our coring sites [22].

Table 1
Location and length of the investigated gravity cores

Core name	Latitude N	Longitude E	Water depth (m)	Core length (cm)
GeoB 7604-2	42°56.2′	30°01.9′	1977	592
GeoB 7607-2	43°09.7′	29°57.7′	1562	636
GeoB 7608-1	43°29.2′	30°11.8′	1202	685
GeoB 7609-1	43°32.8′	30°09.2′	941	655
GeoB 7610-1	43°38.9′	30°04.1′	465	880
GeoB 7616-4	43°41.0′	30°02.5′	168	916
GeoB 7611-1	43°41.8′	30°00.1′	118	634

3. Material and methods

Our study is based on seven gravity cores from the NW Black Sea retrieved during *RV Meteor* cruise M51-4 [23] that are located on a depth transect ranging from the outer shelf to the lower continental slope (Table 1). The cores from the slope (GeoB 7604-2, 7607-2, 7608-1, 7609-1, 7610-1) reveal an undisturbed sequence of the marine units I (finely laminated coccolith ooze) and II (sapropelic sediments) at the top, with a relatively constant combined thickness of ca. 45 cm. The lower parts of the cores consist of homogeneous to (mostly) mm-scale laminated muddy clay (lacustrine unit III). The shelf cores GeoB 7611-1 and GeoB 7616-4 do not contain Holocene sediments (except for a shelly horizon at the top of GeoB 7611-1 with a Late Holocene age of 2585 yr BP) and thus represent nearly entirely the lacustrine unit III. Sedimentologically, the two cores are characterised by mm to cm-scale laminated mud with abundant shells and shell fragments of bivalves and gastropods. All cores listed in Table 1 except GeoB 7611-1 were XRF-

Table 2
Radiocarbon ages for gravity cores GeoB 7608-1 and 7616-4

Lab.-ID	Core depth (cm)	^{14}C age (yr BP)	Calendar age (yr BP)	Material
GeoB 7608-1				
KIA 21464	34	7735 ± 50	7607 ± 40	Ostracods
KIA 21463	88	11,460 ± 70	12,342 ± 215	Gastropod
KIA 21461	158	13,350 ± 80	14,469 ± 365	Gastropod
KIA 21460*	243	17,080 + 150/− 140	18,563 ± 320	Ostracods and bivalves
KIA 21866	436	16,360 ± 70	17,951 ± 285	Ostracods and bivalves
KIA 21459	596	20,140 + 180/− 170	22,499 ± 265	Gastropod
KIA 21457	652	24,970 + 310/− 300	26,891 ± 480	Mixed mollusc shells
GeoB 7616-4				
KIA 18212	2	10,470 ± 60	12,360 ± 200	*Dreissena rostriformis*
KIA 19681	184	10,945 ± 60	12,855 ± 50	*Dreissena rostriformis*
KIA 19680	386	11,250 ± 60	13,055 ± 90	*Dreissena rostriformis*
KIA 19678	579	11,670 ± 80	13,435 ± 140	*Dreissena rostriformis*
KIA 19677	802	12,040 ± 130	13,824 ± 220	*Dreissena rostriformis*
KIA 18213	899	13,105 ± 55	15,452 ± 105	*Dreissena rostriformis*

For GeoB 7608-1 a correction of 1000 yr was applied before calibrating, in GeoB 7616-4 calendar ages were calculated with 0 yr correction. *The date from 243 cm depth in GeoB 7608-1 was discarded because of the high amount of broken and probably reworked shells in the sample.

scanned in high resolution (for further details see Bahr et al. [15]).

The age models of the individual cores have been recently published [15]. They are based on 6 AMS ^{14}C dates for each of the cores GeoB 7608-1 and 7616-4 (Table 2). The age models could be transferred to the other cores through detailed correlations using XRF and colour data (Ti/Ca shown in Fig. 2). For calibration to calendar years BP (1950) we used the program CALPAL (Version 2003 [24]) which uses the INTCAL-98

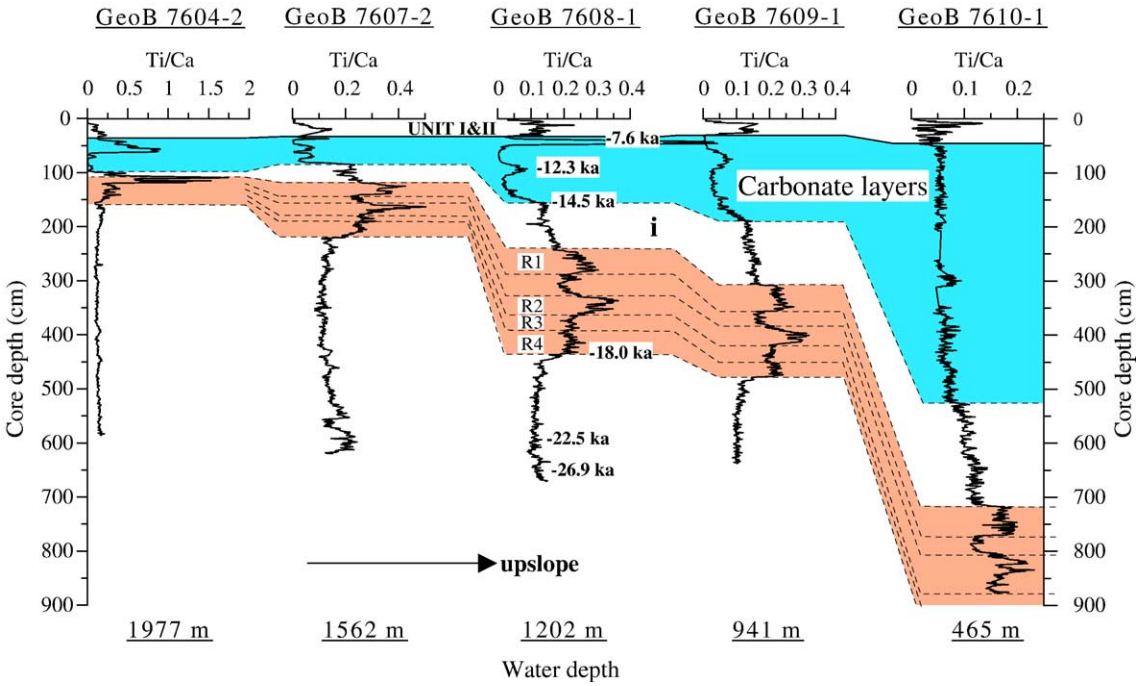

Fig. 2. Correlation of gravity cores from the slope transect in the NW Black Sea using the Ti/Ca ratio. For GeoB 7608-1 the radiocarbon dates are given in calendar years. The rather uniform thickness of the marine unit I contrasts the varying thickness of the red clay layers (in red, labelled R1 to R4) and the carbonate layers (in cyan, see also Ca-peaks in Fig. 4). The interval between the red layers and carbonate layers is labelled as "i". (For interpretation of the references to colour in this figure legend, the reader is referred to the web version of this article.)

[25] calibration set. Based on the correlation with the two published cores BLKS9809 and 9810 [12] (Fig. 3) we calculated calendar years applying a 1000 yr age correction for GeoB 7608-1 and a 0 yr correction for GeoB 7616-4 (for further details see Bahr et al [15]).

For stable isotope analyses ($\delta^{18}O$ and $\delta^{13}C$) on core GeoB 7616-4 a total of 288 samples in 4 cm intervals were collected and wet sieved. Subsequently 5 to 7 juvenile shells of the freshwater bivalve *Dreissena rostriformis* were hand-picked and analysed at the University of Bremen using a Finnigan MAT 251 mass spectrometer with an automated carbonate preparation device. For GeoB 7608-1 we took 319 samples in 2 cm intervals and prepared 5–8 shells of juvenile ostracods belonging to the genus *Candona* spp. (*C. schweyeri* and *C. angulata*) for stable isotope measurements. Additionally a total of 50 samples with *Candona* spp. from the cores GeoB 7604-2, 7607-2, 7609-1 and 7610-1 were analysed. The ratio of $^{18}O/^{16}O$ is given in ‰ relative to the PDB standard. Analytical long-time standard deviation is about ± 0.07‰ PDB and ± 0.26‰ the analytical precision from 18 replicated measurements.

Spectral analyses were performed with the program AnalySeries [26] using the Blackman–Tukey method. This algorithm first computes the autocovariance of the data, applies then a Tukey window and finally computes the power spectrum by Fourier-transforming covariance functions. Before analysing we detrended the data to further pronounce the interannual to decadal variability in the records.

All data are available under the name of the corresponding author through the PANGAEA server (www.pangaea.de/PangaVista).

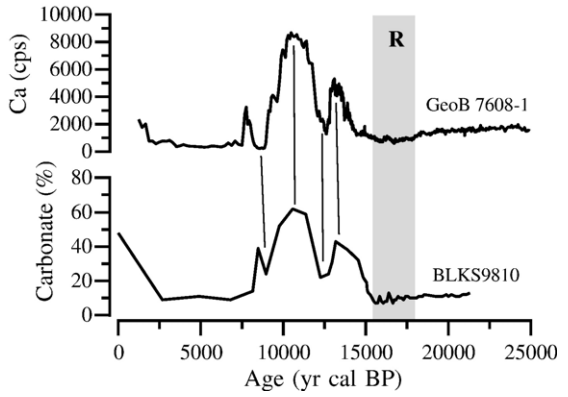

Fig. 3. Correlation of the XRF-Ca content in GeoB 7608-1 from 1202 m water depth and the carbonate content of core BLKS9810 from 378 m (from [12]). For GeoB 7608-1 a 1000 yr age correction was applied before calibrating the radiocarbon dates. BLKS9810 was calibrated to calendar years with a reservoir age correction of 0 yr. R indicates the occurrence of reddish-brown clay layers.

4. Results

4.1. Sedimentological characteristics

A detailed description of the sedimentological characteristics of GeoB 7608-1 was already given in Bahr et al. [15], thus only a short overview over the most important features will be presented here. Sedimentological data including the Ti and Ca-intensity and bulk grain size from GeoB 7608-1 for the time interval of 5 to 28.5 kyr BP are presented in Fig. 4.

The Ti and Ca contents mainly reflect the varying contribution of biogenic and/or authigenic precipitated calcite (Ca) versus siliciclastic terrigenous input (Ti). After a period of rather constant Ti and Ca intensities before ca. 18.5 kyr BP, the terrigenous input (represented by high Ti) increases sharply until ca. 15.5 kyr BP, equivalent to a series of four distinct reddish-brown clay-layers. About 1000 yr later, contemporaneous to the Bølling warm period, the Ca intensity shows the first of three separated maxima, reflecting high amounts of authigenically precipitated calcite.

Sand content is as high as 2.4% until 26 kyr BP but steadily drops to values between 0.2% and 1% during the red layer deposition. The grain size rises subsequently towards a first maximum (up to 3.6 wt.%) which terminates abruptly at the onset of the Bølling at 14.5 kyr BP; a second maximum (3.6 wt.%) could be observed during the lower Ca-trough, contemporaneous to the Younger Dryas (YD).

The cores from the slope (except GeoB 7616-4) could be correlated using XRF and colour scan data (Ti/Ca is shown in Fig. 2). In contrast to the Holocene units I and II, that have a fairly constant thickness in all cores, the sedimentation rate of the limnic sediments increases at least fourfold towards shallower water depths. This increase is most pronounced in the interval between the end of the red layers and the onset of the carbonate peaks, but is less pronounced during the deposition of the red layers (Fig. 2).

4.2. Stable isotopes

Ostracods are widely used for reconstructing paleoenvironmental changes, especially in lakes. It is known that ostracods do not calcify in equilibrium with the ambient water but show constant, temperature-independent offsets. Von Grafenstein et al. [27] calculated this offset to be +2.2 ± 0.15‰ for all Candoninae with respect to the equilibrium calcite. Because of the scarcity of material in our cores we had to combine juvenile instars (A-1 to A-4; A-1 refers to the juvenile stage

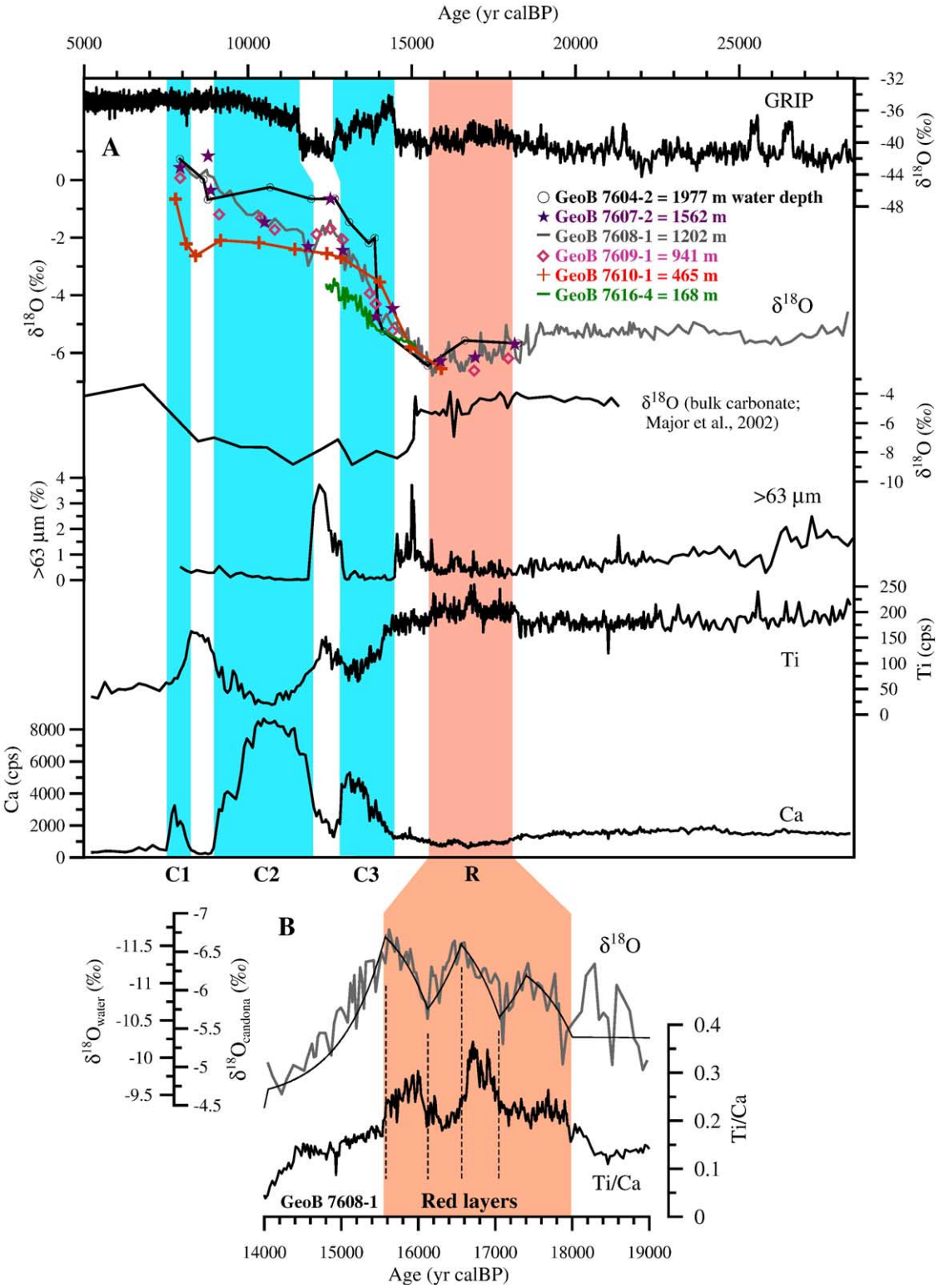
Age (yr calBP)
5000
10000
15000
20000
25000
A
GRIP
δ18O (‰)
-32
-36
-40
-44
-48
0
-2
-4
-6
○ GeoB 7604-2 = 1977 m water depth
★ GeoB 7607-2 = 1562 m
GeoB 7608-1 = 1202 m
◇ GeoB 7609-1 = 941 m
+ GeoB 7610-1 = 465 m
GeoB 7616-4 = 168 m
δ18O
δ18O (bulk carbonate; Major et al., 2002)
-4
-6
-8
-10
>63 µm (%)
4
3
2
1
0
>63 µm
250
200
150
100
50
0
Ti (cps)
Ti
8000
6000
4000
2000
0
Ca (cps)
Ca
C1
C2
C3
R
B
δ18Owater (‰)
-7
-6.5
-6
-5.5
-5
-4.5
-11.5
-11
-10.5
-10
-9.5
δ18Ocandona (‰)
δ18O
0.4
0.3
0.2
0.1
0
Ti/Ca
Ti/Ca
GeoB 7608-1
Red layers
14000
15000
16000
17000
18000
19000
Age (yr calBP)

prior to adulthood, A-2 to the previous stage etc.) of different species of *Candona* (*C. schweyeri* and *C. angulata*) in one sample, assuming the same vital offset for all species.

$\delta^{18}O$ measurements on juvenile *Candona* spp. from GeoB 7608-1 (Fig. 4A) reveal a relatively stable level during the glacial interval of our records with values around −5.6‰ between 28 and 25 kyr and −5.2‰ BP between 25 and 18.5 kyr BP. A significant depletion is observed during the deposition of the red layers between 18.5 and 15.5 kyr BP, where $\delta^{18}O$-values decrease down to −6.5‰. The distinct terrigenous pulses during this period [15] are mirrored by the almost contemporaneous negative peaks in the $\delta^{18}O$-record. After 15.5 kyr BP values start to increase and reach their LGM-level with the onset of the Bølling warm period. Thereafter, we observe a stepwise shift towards enriched values. The steepest increase (from −5.0‰ to −1.95‰) takes place between 14.0 and 12.9 kyr BP, followed by a period of more stable values between 12.9 and 11.1 kyr BP including two significant negative excursion of −3.0‰ at ca. 12.9 and 11.8 kyr BP. Finally, $\delta^{18}O$ increases from −1.75‰ at 11.1 kyr BP towards +0.68‰ at 8 kyr BP.

$\delta^{18}O$ values measured on *D. rostriformis* juv. from GeoB 7616-4 show a general increasing trend from −5.7‰ at ca. 15.2 kyr BP towards heavier values around −3.5‰ at 12.5 kyr BP but are highly variable with fluctuations of ~1‰ or more on multidecadal and centennial time-scales.

Comparing the major trends in $\delta^{18}O$ at different water depths, the records appear to diverge since ca. 14.5 kyr BP. While cores from intermediate water depths (1562 to 465 m) have $\delta^{18}O$ values in the range of GeoB 7608-1 (1202 m), the shallow core GeoB 7616-4 (168 m) shows a trend to values up to 1.5‰ lighter than GeoB 7608-1. $\delta^{18}O$ from the deepest core GeoB 7604-2 (1977 m), on the other hand, is up to 2‰ heavier than those in GeoB 7608-1 since 14.5 kyr BP. This difference diminishes between 9 and 8 kyr BP where the $\delta^{18}O$-records seem to merge. Another diverging trend is noticeable since ca. 12.5 kyr BP, when GeoB 7610-1 from 465 m water depth starts to show depleted values relative to GeoB 7608-1.

5. Discussion

By combining our isotope records at different water depths with sedimentological evidence [15], we can provide a detailed picture of the hydrological evolution of the Black Sea over the last glacial and deglaciation. In addition, high resolution isotope data from the shelf core GeoB 7616-4 allow to discuss short-term fluctuations during the Bølling/Allerød (B/A) and YD intervals.

5.1. The paleohydrological evolution of the Black Sea

5.1.1. Evolution between 28.5 to 14.5 kyr BP

Beside of some minor fluctuations, the stable $\delta^{18}O$ record before 18.5 kyr BP indicates that the Black Sea was in a state of isotopic equilibrium. This steady state was terminated by the observed 1‰-drop in $\delta^{18}O$ between ca. 18 and 15 kyr BP. During the time of the red layer deposition the Scandinavian Ice Sheet dammed large lakes and diverted rivers and meltwater drainage southward towards the River Volga and into the Caspian Sea. These (melt)waters caused the Caspian Sea to overflow over the Manych depression (+26 m a.s.l.) into the Black Sea [13,14]. The low $\delta^{18}O$ values observed in the Black Sea could therefore be explained by the contribution of this isotopically depleted water. On a finer scale, the observed changes in the ostracod oxygen isotopes are characterised by a saw-tooth pattern (Fig. 4B). The $\delta^{18}O$ values are getting gradually more depleted during each phase of meltwater input (displayed by a high Ti/Ca ratio), but rise again relatively rapidly when the meltwater supply ceases (low Ti/Ca). This leads to apparent lags of the maxima and minima in the $\delta^{18}O$ data relative to the Ti/Ca record, reflecting the time the Black Sea basin needs to adjust to hydrological changes. The tendency towards heavier isotopic values after the termination of each meltwater inflow is related to the temporary reduction of the meltwater inflow.

Fig. 4. (A) $\delta^{18}O$ data (uncorrected for vital offsets) measured on *Candona* spp. from cores GeoB 7604-2, 7607-2, 7608-1, 7609-1, 7610-1, and 7616-4 (measured on *D. rostriformis* juv., 7-point running average), $\delta^{18}O$ (bulk) from core BLKS9810 [12]; bulk sand content, XRF Ti and Ca-intensity measured on core GeoB 7608-1 from the NW Black Sea slope and their suggested correlation with the GRIP ice-core $\delta^{18}O$ record. Marked are the occurrence of the red clay layers (R) and the Ca-peaks (C1–3). Note the different scale used for $\delta^{18}O$ of bulk carbonate and shell material. (B) Ostracod $\delta^{18}O$ record from core GeoB 7608-1 (grey line), modelled $\delta^{18}O$ of the Black Sea water (black line) and XRF Ti/Ca ratio from GeoB 7608-1 for the interval covering the red layer deposition. Red shading shows the termination of the red layers; dashed lines border the periods with peak Ti/Ca ratio that were incorporated into the isotopic balance model (see Table 3 for details). The scale for $\delta^{18}O_{water}$ was adjusted to the corresponding values of $\delta^{18}O_{ostracod}$, calculated for a constant water temperature of 4 °C. (For interpretation of the references to colour in this figure legend, the reader is referred to the web version of this article.)

To assess the sensitivity of the Black Sea towards changes in amount and isotopic composition of river run-off, we performed a simple mass balance calculation. Our model is primarily based on the considerations underlying the hydrologic-isotope-balance model (HIBAL) by Benson and Paillet [28], although with the simplification that we assumed a fully mixed Black Sea with a constant volume for the period prior to 14.5 kyr BP and the simulations were run by year not by month (boundary conditions are summarised in Table 3). Considering the values used for computing the pre-red layer steady state, it is striking that a very negative $\delta^{18}O_{run\text{-}off}$ is needed to reach the ca. −10.2‰ for $\delta^{18}O_{water}$. This might be explained by a greater portion of isotopic depleted water entering the Black Sea from the northern drainage area.

It becomes apparent that a relatively small change in run-off and $\delta^{18}O_{run\text{-}off}$ is sufficient to simulate the magnitude of the observed isotopic excursions (Table 3; Fig. 4B). To compare both model and observation we calculated $\delta^{18}O_{ostracod}$ from the modelled $\delta^{18}O$ of the Black Sea water using the formula [29]

$$\delta^{18}O_{ostracod} = (2.6229 \cdot 10^{6} \cdot (273.15 + T)^{-2} + 0.97002 \cdot \delta^{18}O_{water} - 31.7648) + 2.2;$$

T was set to 4 °C, $\delta^{18}O_{ostracod}$ is given relative to the PDB standard, $\delta^{18}O_{water}$ to SMOW.

The two negative $\delta^{18}O$-excursions before the start of the red layer interval indicate that there must be a second source (e.g., Dnestr and Dnepr) for isotopic depleted water beside the one that is responsible for the red clays.

As proposed by other authors [2,30,31], the Black Sea could have possibly spilled via the Sea of Marmara into the Aegean Sea during this time. This scenario is supported by studies of dinoflagellate cysts, freshwater algae and fungal spores [32] that suggest freshwater to brackish conditions in the Sea of Marmara during this period.

The $\delta^{18}O$ values of all cores GeoB 7604-2, 7607-2, 7609-1 and 7610-1 are in the range of GeoB 7608-1, implying that the lake has not been stratified. Bahr et al. [15] suggested that a stratification of the ancient Black Sea is responsible for the persistent 1000-yr age correction in our age model. As shown in the following section, this might be the case after 14.5 kyr BP; however, the $\delta^{18}O$ record does not support this assumption for the period before 14.5 kyr BP.

5.1.2. Evolution between 14.5 to 8 kyr BP

The pronounced trend towards heavier values for $\delta^{18}O$ in GeoB 7608-1 since the end of the red layers is primarily the effect of increasing $\delta^{18}O$ of run-off and on-lake precipitation as well as enhanced evaporation. The well-documented 3.5‰ increase in $\delta^{18}O$ of atmospheric precipitation between Oldest Dryas and B/A in central Europe [33] could almost account alone for the whole shift of ca. 4‰ that occurred in our record since the end of the red layer period and the begin of the YD. It is therefore not surprising that the return to almost LGM-values in $\delta^{18}O_{prec}$ during the YD [33] interrupted the increasing $\delta^{18}O$ trend in core GeoB 7608-1. The $\delta^{18}O$-peak at the end of the YD is questionable, because it consists only of one measurement. Nevertheless, remeasuring confirmed this value and GeoB 7607-2 shows also a value almost as low as in 7608-1. The peak occurred shortly after the maximum in bulk grain size, thus seems no to be related to high river discharge and freshwater input. On the other hand, alpine lake level records show a short (200 to 300 yr) phase of high lake level at the YD termination (the so-called Onoz 3 phase at ca. 11.7 kyr BP [34]) what might argue in favour of a highly increased run-off at that time.

Table 3
Hydrologic and climatic boundary conditions for the isotopic balance model

Time slice (kyr BP)	V (km^3)	Q_r (km^3 yr^{-1})	$\delta^{18}O_r$ (‰)	Q_p (km^3 yr^{-1})	$\delta^{18}O_p$ (‰)	Q_e (km^3 yr^{-1})	T (°C)	h (%)
25–18	537,000	450	−20	230	−11.5	205	4	76
18–17.4	537,000	550	−21.5	230	−11.5	230	4	76
17.4–15[a]	537,000	570	−22.3	230	−11.5	230	4	76
17.4–15[b]	537,000	460	−20.2	230	−11.5	230	4	76
15–14.5	537,000	450	−20	230	−11.5	240	4	76
Modern[c]	537,000	350	−10	230	−8	280	11.2	78

V — lake volume; Q_r — volume of run-off; $\delta^{18}O_r$ — $\delta^{18}O$ of run-off; Q_p — volume of on-lake precipitation; $\delta^{18}O_p$ — $\delta^{18}O$ of precipitation; Q_e — volume of evaporation; T — temperature of lake surface; h — relative humidity.

[a] Values for periods with peak Ti/Ca (see Fig. 4).

[b] Values for periods with average Ti/Ca (see Fig. 4).

[c] Values from [43].

The in relation to the other cores relatively heavy δ^{18}O-values from the deepest core GeoB 7604-2 (1977 m water depth) strongly suggest the existence of a denser bottom layer in the Black Sea during the B/A warm period, most likely produced through evaporation accompanied by biogenic calcite-precipitation forming the Ca-peaks (Fig. 4A). Another supporting evidence for increased evaporation as a cause for deep water formation is a sudden decrease in δ^{18}O of bulk carbonate at ca. 15 kyr BP [12] (Fig. 4A). The carbonate fraction mostly consists of authigenically precipitated calcite produced by high phytoplankton activity [12,15] — low δ^{18}O of bulk carbonate should therefore reflect higher temperatures.

Although the values and the trend in δ^{18}O of core GeoB 7604-2 are decoupled from the shallower cores until 9 to 10 kyr BP no clear evidence for permanent anoxia could be identified in the deepest core GeoB 7604-2. This indicates that oxygen supply by deep-water formation must have been sufficient. The different trends observed in GeoB 7604-2 and the intermediate cores could mirror different rates of mixing. While a relatively small volume of deep water (presumably well below 1562 m water depth, where GeoB 7607-2 is located) would adjust relatively quickly to the increased $\delta^{18}O_{prec}$ and salinity, the upper water body reacts less rapidly to these changes due to its much larger volume. Thus, the deep water -δ^{18}O of 7604-2 reaches more or less constant values around −0.6‰ as early as 12.5 kyr BP, while in 7608-1 such values are observed later (at ca. 9.5 kyr BP).

While cores GeoB 7607-2, 7608-1, 7609-1, and 7610-1 show comparable values during the B/A, GeoB 7616-4 exhibits a trend towards lighter δ^{18}O at least since ca. 14 kyr BP. Although it should be noted that the values are measured on bivalve shells and not on ostracod valves, potential vital offset between both benthic organisms should not affect the trends observed in δ^{18}O. Increasing temperatures would counteract the trend towards heavier δ^{18}O values in GeoB 7616-4, since it is located in a relatively shallow water depth of 168 m or perhaps an even shallower one, if the Black Sea level was lowered during the B/A by evaporative drawdown [12]. A second important factor is the influence of the Danube's freshwater plume, which today leads to a depletion of δ^{18}O values on the NW Black Sea shelf (see Section 2). The trend towards isotopic values lighter than those in the deeper cores might point to a progradation of the delta to the shelf edge during a period of low sea level, shifting GeoB 7616-4 gradually to a more proximal position to the freshwater source, thus enhancing the influence of the Danube. The assumption of a low lake level and a progradation of the Danube delta is further corroborated by the strong upslope increase of the sedimentation rates during the deposition of the lowermost Ca-peak [15].

Another question is connected to the cause for the lighter δ^{18}O values of core GeoB 7610-1 relative to the deeper cores since the YD: Although 7610-1 is located closer to the Danube delta than the deeper cores, it seems on the first sight unlikely that increased freshwater influence plays a major role, because in this case core GeoB 7610-1 should also have shown a trend towards lighter values relative to the other cores as observed in the shallowest core 7616-4 during B/A, where a proximal position to the Danube is proposed to have lowered the local δ^{18}O signal (see above). Increased water temperatures in the upper 465 m (or less, if the lake level was considerably reduced during this period [12]) might have lowered the δ^{18}O of GeoB 7610-1. The difference between δ^{18}O in core GeoB 7610-1 and core GeoB 7608-1 from 1202 m water depth is 2‰ at maximum (or even 2.7‰ at 8.7 kyr BP), which would account for a temperature difference of ca. 8 to 10.8 °C. This seems to be unrealistically high, a combination of both temperature and Danube-influence might account for the whole difference.

5.2. High-frequent variability of the Danube's discharge during the late glacial

Today, the Danube river run-off is closely linked to the North Atlantic Oscillation (NAO) [35,36], which exerts a strong influence on the precipitation-pattern over Europe on interannual to decadal time scales. Our high-resolution records obtained on the shallow core GeoB 7616-4 provide a good opportunity to determine if there is any evidence that a NAO-like climatic mode also prevailed during the last deglaciation.

In Section 5.1.2. we argued that core GeoB 7616-4 is under direct influence of the freshwater input by the Danube. In fact, the high variability in its δ^{18}O-record most likely mirrors pronounced short-term oscillations in the Danube's discharge. This assumption is based on the comparison of the δ^{18}O record and grain size fluctuations from this core. Negative excursions in δ^{18}O, interpreted to represent freshwater pulses, often correspond to positive excursions in the sand content, which are thought to represent maxima in the fluvial input (Fig. 5A). A spectral coherency calculation between both records shows that the main common periodicity at the 95% confidence level is 65 yr, with a ca. 180° phase lag (the sampling interval lies between 7 and 11 yr and is therefore sufficient to resolve a peri-

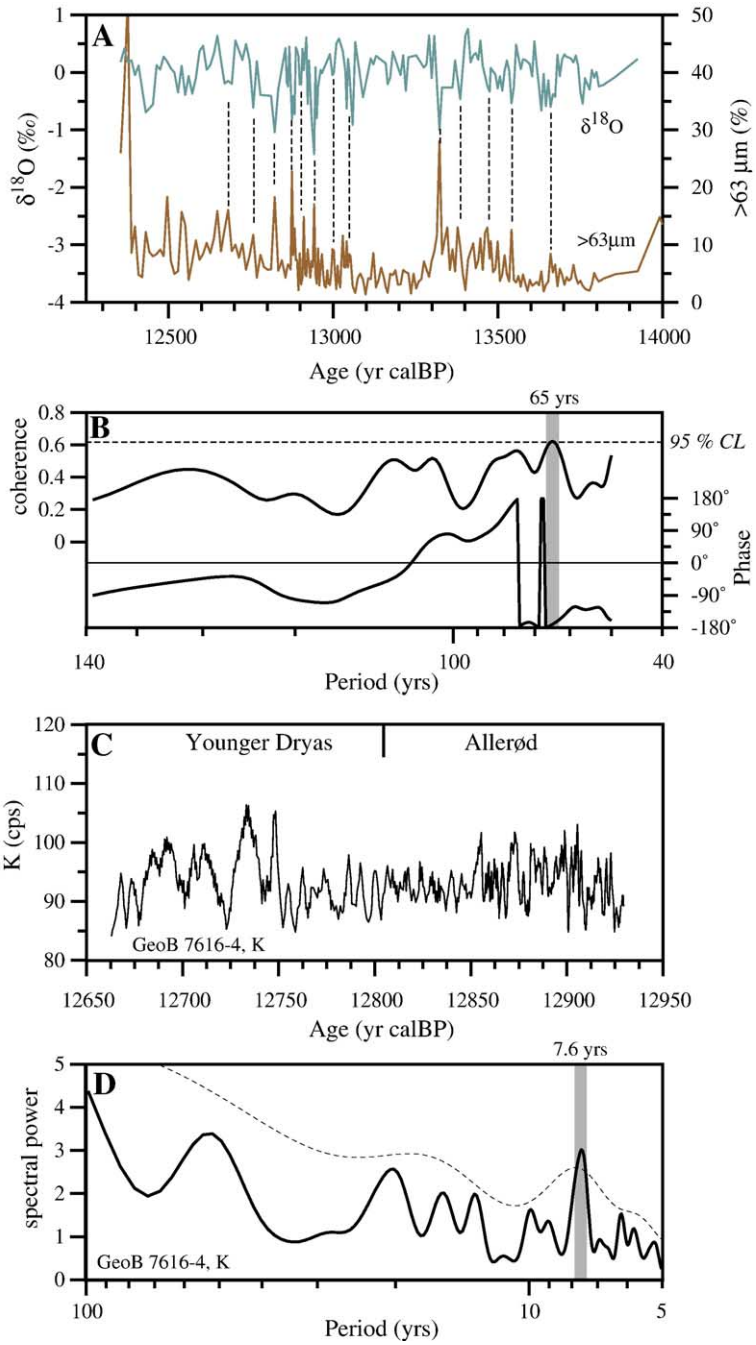

Fig. 5. (A) δ^{18}O values (detrended through subtraction from a 60 point adjacent average) measured on *Dreissena rostriformis* juv. and bulk sand content from GeoB 7616-4. Dashed lines delineate peaks of high sand content (high fluvial discharge) that correspond to negative excursions in the δ^{18}O record (lowered salinity). (B) Blackman–Tukey cross-spectral coherence and phasing between δ^{18}O and sand content at the 95% confidence level. The major coherent phase of 65 yr with a ca. 180° phasing is indicated. CL indicates "confidence level". (C) 5-point average of K measured in 2 mm intervals on a section of core GeoB 7616-4. Please note the different time scales used in (A) and (C). (D) Blackman–Tukey spectrum of the detrended K values from core GeoB 7616-4 for the interval between 12,659–12,931 yr BP. Analyses were performed with the Analyseries software [26] using a 0.5 yr sampling interval, 272 lags and 0.01103 bandwidth (straight line: one sided confidence interval at the 80% level) and 54 lags and 0.05558 bandwidth (dashed line: low-resolution spectrum). Indicated is the major NAO-related 7.6 yr-period.

odicity of 65 yr), consistent with the above mentioned inverse correlation between sand content and $\delta^{18}O$. This 65 yr cyclicity falls within the range of the 65–70 yr periodicity of the North Atlantic Ocean/Northern Hemisphere climate system described by Schlesinger and Ramankutty [37].

Beside this multidecadal variability, a closer inspection of a section with cm-scale alternations of coarse and fine grained material in core GeoB 7616-4 using XRF-measurements in 2 mm (equivalent to 0.2–0.5 yr) resolution, reveals prominent multiannual fluctuations, as shown for example in the K record (Fig. 5B). Those fluctuations are caused by the different mineralogy of the quartz-rich coarse grained layers with a low K-concentration, and the finer grained layers with abundant mica and clay minerals and therefore high K-content. Spectral analyses of our high-resolution XRF data show a significant peak at 7.6 yr in the Ca, Fe, Ti and K records (K is presented in Fig. 5C), which is also the most prominent period in the instrumental NAO-record [38]. The presence of the 7.6 and 65 yr periods suggests that major modern modes of North Atlantic climate variability on interannual to decadal time scales affected the precipitation pattern of SE Europe likewise during the deglacial period. Additionally, the North Atlantic was also at least during parts of the deglacial period a region that exerted a major influence on the central European climate. Although the fact that the North Atlantic drives the European climate is not unexpected, the persistence of modern-day climatic features during noticeably different climatic periods is remarkable.

5.3. Implications for the timing of the first inflow of marine water into the Black Sea

Regarding the question when the reconnection of the Black Sea with the Mediterranean Sea started, it has been proposed that the Bosphorus sill was deeper than present (around −80 m [39] or even −100 m [3]) before the flooding of the Black Sea, thus allowing an inflow of saline waters as early as 14 kyr BP. This scenario would be consistent with the divergence of $\delta^{18}O$ values in the deepest core GeoB 7604-2 that become about 1.8‰ heavier at this time (Fig. 4A). Hydrological calculations [3] however showed that this idea seems unlikely with respect to the first occurrence of marine fauna in the Sea of Marmara at around 13.7 kyr BP [40,41] and the onset of sapropel development in the Black Sea as late as 7500 yr BP [42]. Salinification of the Sea of Marmara at 13.7 kyr BP requires a low freshwater outflow from the Black Sea. If this was the case, a −80 m (or −100 m) deep Bosphorus sill would permit a salinification of the Black Sea at around 11.0 to 11.8 kyr BP, a long time before the onset of sapropel development. A high outflow of freshwater from the Black Sea into the Sea of Marmara would have delayed the salinification of the Black Sea to a more reasonable date, but would have also prevented Mediterranean water from entering the Sea of Marmara postponing the salinification of the Sea of Marmara to a considerable time after 13.7 kyr BP, which contradicts the faunal evidence [40,41].

The continuity of the trend towards heavier $\delta^{18}O$ in GeoB 7608-1 argues against the proposed catastrophic flooding of the Black Sea around 9.5 kyr BP [2]. The $\delta^{18}O$ in the Sea of Marmara at 9.5 kyr BP is +0.88‰ [10] measured on the planktic foraminifera *Turborotalita quinqueloba*, or an expected +3.08‰ for our record, if the vital offset of +2.2 for Candoninae is taken into consideration. Thus the inflow of considerable amounts of isotopic enriched Mediterranean water should enhance the trend towards heavier $\delta^{18}O$ values. This is not the case in core GeoB 7608-1 (Fig. 4A) but might be visible in pronounced positive shifts observed in the $\delta^{18}O$ records of the deepest cores GeoB 7604-2 and 7607-2 at ca. 9 kyr BP. It is suggestive to interpret this as a sign for dense Mediterranean water entering the deep Black Sea, but the paucity of data points makes this assumption very speculative. Additionally, the records from cores GeoB 7604-2, 7607-2, 7609-1 and especially 7610-1 show a steeper trend towards heavier $\delta^{18}O$ since ca. 9 kyr BP. The striking increase of $\delta^{18}O$ since 8.5 kyr BP recorded in GeoB 7610-1 seems to be related to the accompanying rise of the Black Sea level that diminishes the influence of depleted $\delta^{18}O$ water delivered by the Danube at this core location (see Section 5.1.2.).

If, however, the reconnection started around 9.5 kyr BP in a more gradual manner, the merging of the $\delta^{18}O$ records from GeoB 7604-2, 7607-2, 7608-1, 7609-1 and 7610-1 could be interpreted as a result of a homogeneous water column during the first inflow of saline water. The timing of the general $\delta^{18}O$ increase also corresponds to higher sea-surface salinity in the Sea of Marmara [10] after 9.5 kyr BP that was interpreted to be the result of an increased amount of saline Mediterranean water flowing through the Sea of Marmara during the flooding of the Black Sea [10]. Although a homogenized water column requires a strong inflow of Mediterranean waters and deep mixing, the rate of $\delta^{18}O$-change itself does not appear to be high enough to support a catastrophic infill of the Black Sea within a few years.

6. Conclusions

The combination of high resolution $\delta^{18}O$ records, XRF and grain size measurements reveal the following pattern of Black Sea hydrological evolution since the Last Glacial Maximum:

After overall stable conditions during the LGM between 15.5 and 18.5 kyr BP a series of meltwater pulses derived from Scandinavian ice sheets led to a 1‰-depletion in the $\delta^{18}O$ of the Black Sea. After this interval, at the onset of the Bølling/Allerød warm period enriched $\delta^{18}O$ of atmospheric precipitation led to a gradual increase in the oxygen isotope composition of the Black Sea from −6.7‰ to +0.6‰, only interrupted by more constant values during the Younger Dryas cold period.

Comparison of $\delta^{18}O$-records from cores located at water depths between 168 to 1977 m along the slope showed that all record have similar values until 14.5 kyr BP, when the deepest core from 1977 m water depth starts to show $\delta^{18}O$ values at least 1‰ heavier than in the intermediate cores. This indicates the formation of isotopic enriched deep water through evaporation during warm climatic conditions which is also expressed in high amounts of authigenic precipitated calcite. The shallowest cores from 168 and 465 m water depth on the other hand show a tendency towards lighter values compared to the deeper cores since 14.5 and ca. 12.5 kyr BP, respectively. Those trends might reflect increasing temperatures in the upper water column and an enhanced freshwater influence by the Danube during a period of lowered Black Sea lake level. High-frequent variations in the run-off of the Danube during the Younger Dryas and the Bølling indicate that a NAO-like climate mode may have governed the interannual to decadal variability also during the last deglaciation.

At 9.5 kyr BP stable oxygen isotope values from all investigated sediment cores start to merge, indicating that during the beginning inflow of saline Mediterranean waters the water column of the Black Sea was probably homogenous. However, the rate of change in $\delta^{18}O$ at this point does not support any catastrophic infill of the Black Sea within only a few years.

Acknowledgements

We thank captain and crew of the *RV Meteor* for their efficient support during Meteor cruise M 51-4. We also thank M. Segl, University of Bremen, and her team for performing the stable isotope analysis and U. Röhl, University of Bremen, for support in XRF measurements. We also gratefully acknowledge the help of Ian Boomer with identifying the ostracods. The manuscript benefited from the comments of three anonymous reviewers and the editor H. Elderfield. This research was founded by the Deutsche Forschungsgemeinschaft grants no. LA 1273/2-1, LA 1273/2-2, and WE 992/47-3. No. RCOM0346.

References

[1] W.B.F. Ryan, W.C. Pitman III, C. Major, K. Shimkus, V. Moskalenko, G.A. Jones, P. Dimitrov, N. Görür, M. Sakinc, H. Yüce, An abrupt drowning of the Black Sea shelf, Mar. Geol. 138 (1997) 119–126.

[2] W.B.F. Ryan, C. Major, G. Lericolais, S. Goldstein, Catastrophic flooding of the Black Sea, Annu. Rev. Earth Planet. Sci. 31 (2003) 525–554.

[3] P.G. Myers, C. Wielki, S.B. Goldstein, E.J. Rohling, Hydraulic calculations of postglacial connections between the Mediterranean and the Black Sea, Mar. Geol. 201 (2003) 253–267.

[4] G.F. Lane-Serff, E.J. Rohling, H.L. Bryden, H. Charnock, Postglacial connection of the Black Sea to the Mediterranean and its relation to the timing of sapropel formation, Paleoceanography 12 (1997) 169–174.

[5] M. Siddall, L.J. Pratt, K.J. Helfrich, L. Giosan, Testing the physical oceanographic implications of the suggested sudden Black Sea infill 8400 years ago, Paleoceanography 19 (2004) PA 1024.

[6] P.J. Mudie, A. Rochon, A.E. Aksu, Pollen stratigraphy of Late Quaternary cores from Marmara Sea: land-sea correlation and paleoclimatic history, Mar. Geol. 190 (2002) 233–260.

[7] A.E. Aksu, R.N. Hiscott, D. Yasar, F.I. Isler, S. Marsh, Seismic stratigraphy of Late Quaternary deposits from the southwestern Black Sea shelf: evidence for non-catastrophic variations in sea-level during the last 10000 yr, Mar. Geol. 190 (2002) 61–94.

[8] A.E. Aksu, R.N. Hiscott, M.A. Kaminski, P.J. Mudie, H. Gillespie, T. Abrajano, D. Yasar, Last glacial–Holocene paleoceanography of the Black Sea and Marmara Sea: stable isotopic, foraminiferal and coccolith evidence, Mar. Geol. 190 (2002) 119–149.

[9] R.D. Ballard, D.F. Coleman, G.D. Rosenberg, Further evidence of abrupt Holocene drowning of the Black Sea shelf, Mar. Geol. 170 (2000) 253–261.

[10] M. Sperling, G. Schmiedl, C. Hemleben, K.C. Emeis, H. Erlenkeuser, P.M. Grootes, Black Sea impact on the formation of eastern Mediterranean sapropel S1? Evidence from the Marmara Sea, Palaeogeogr. Paleaeoclimatol. Palaeoecol. 190 (2003) 9–21.

[11] W.G. Deuser, Late-Pleistocene and Holocene history of the Black Sea as indicated by stable isotope studies, J. Geophys. Res. 77 (1972) 1071–1077.

[12] C. Major, W. Ryan, G. Lericolais, I. Hajdas, Constraints on Black Sea outflow to the Sea of Marmara during the last glacial–interglacial transition, Mar. Geol. 190 (2002) 19–34.

[13] Y.G. Leonov, Y.A. Lavrushin, M.P. Antipov, Y.A. Spridonovba, Y.V. Kuzmin, E.J.T. Jull, S. Burr, A. Jelinowska, F. Chalie, New age data on sediments of the transgressive phase of the Early Khvalyn transgression of the Caspian Sea, Dokl. Earth Sci. 386 (2002) 748–751.

[14] J. Mangerud, M. Jakobsson, H. Alexanderson, V. Astakhov, G.K.C. Clarke, M. Henriksen, C. Hjort, G. Krinner, J.P. Lunkka,

P. Möller, A. Murray, O. Nikolskaya, M. Saarnisto, J.I. Svendsen, Ice-dammed lakes and rerouting of the drainage of northern Eurasia during the last glaciation, Quat. Sci. Rev. 23 (2004) 1313–1332.
[15] A. Bahr, F. Lamy, H. Arz, H. Kuhlmann, G. Wefer, Late glacial to Holocene climate and sedimentation history in the NW Black Sea, Mar. Geol. 214 (2005) 309–322.
[16] M. Elliot, L. Labeyrie, T. Dokken, S. Manthé, Coherent patterns of ice-rafted debris deposits in the Nordic regions during the last glacial (10–60 ka), Earth Planet. Sci. Lett. 194 (2001) 151–163.
[17] E. Özsoy, Ü. Ünlüata, Oceanography of the Black Sea: a review of some recent results, Earth Sci. Rev. 42 (1997) 231–272.
[18] N. Panin, D. Jipa, Danube River sediment input and its interaction with the northwestern Black Sea, Estuar. Coast. Shelf Sci. 54 (2002) 551–562.
[19] C. Bondar, I. Stare, D. Cernea, E. Harabagiu, Water flow and sediment transport of the Danube at its outlet into the Black Sea, Meteorol. Hydrol. 21 (1991) 21–25.
[20] T. Oguz, S. Besiktepe, Observations on the Rim current structure, CIW formation and transport in the western Black Sea, Deep-Sea Res. I 46 (1999) 1733–1754.
[21] W. Murray, H.W. Jannasch, S. Honjo, F. Anderson, W.S. Reeburgh, Z. Top, E. Friederich, L.A. Codispoti, E. Izdar, Unexpected changes in the oxic/anoxic interface in the Black Sea, Nature 338 (1989) 411–413.
[22] E. Öszoy, D. Rank, I. Salihoglu, Pycnocline and deep mixing in the Black Sea: stable isotope and transient tracer measurements, Estuar. Coast. Shelf Sci. 5 (2002) 621–629.
[23] B.B. Jørgensen, METEOR-Berichte, Cruise 51, Leg 4, Istanbul–Istanbul, METEOR-Berichte 031-1, Leitstelle METEOR, Hamburg, 2003, 57 pp.
[24] B. Weninger, O. Jöris, CALPAL version 2003 (software), Cologne University, Germany, 2003.
[25] M. Stuiver, P.J. Reimer, E. Bard, J.W. Beck, G.S. Burr, K.A. Hughen, B. Kromer, G. McCormac, J. van der Plicht, M. Spurk, INTCAL98 radiocarbon age calibration, 24,000–0 cal BP, Radiocarbon 40 (1998) 1041–1084.
[26] D. Paillard, L. Labeyrie, P. Yiou, Macintosh program performs time-series analysis, Trans. Am. Geophys. Union 77 (1996) 379.
[27] U. von Grafenstein, H. Erlenkeuser, P. Trimborn, Oxygen and carbon isotopes in modern fresh-water ostracod valves: assessing vital offsets and autecological effects of interest for palaeoclimate studies, Palaeogeogr. Palaeoclimatol. Palaeoecol. 148 (1999) 133–152.
[28] L. Benson, F. Paillet, HIBAL: a isotopic-hydrologic-balance model for application to paleolake systems, Quat. Sci. Rev. 21 (2002) 1521–1539.
[29] H.J. Rösler, H.J. Lange, Geochemische Tabellen, Ferdinand Enke Verlag, Stuttgart, 1976, 674 pp.
[30] D.D. Kvasov, Late Quaternary History of Major Lakes and Inland Seas of Eastern Europe, Nauka, Leningrad, 1975, 248 pp.
[31] A.D. Smith, T. Taymaz, F. Oktay, H. Yuce, B. Alpar, H. Basaran, J.A. Jackson, S. Kara, M. Simsek, High resolution seismic reflection profiling in the Sea of Marmara (north-west Turkey): Late Quaternary sedimentation and sea-level changes, Geol. Soc. Amer. Bull. 107 (1995) 923–936.
[32] P.J. Mudie, A. Rochon, A.E. Aksu, H. Gillespie, Dinoflagellate cysts, freshwater algae and fungal spores as salinity indicators in Late Quaternary cores from Marmara and Black seas, Mar. Geol. 190 (2002) 203–231.
[33] U. von Grafenstein, H. Erlenkeuser, A. Brauer, J. Jouzel, S.J. Johnsen, A mid-European decadal isotope–climate record from 15,500 to 5000 years BP, Science 284 (1999) 1654–1657.
[34] M. Magny, J. Guiot, P. Schoellammer, Quantitative reconstruction of Younger Dryas to Mid-Holocene paleoclimates at Le Locle, Swiss Jura, using pollen and lake-level data, Quat. Res. 56 (2001) 170–180.
[35] E.V. Stanev, E.L. Peneva, Regional sea level response to global climatic change: Black Sea examples, Glob. Planet. Change 32 (2002) 33–47.
[36] N. Rîmbu, C. Boroneant, C. Buta, M. Dima, Decadal variability of the Danube river flow in the lower basin and its relation with the North Atlantic oscillation, Int. J. Climatol. 22 (2002) 1169–1179.
[37] M.E. Schlesinger, N. Ramankutty, An oscillation in the global climate system of period 65–70 years, Nature 367 (1994) 723–726.
[38] J.W. Hurrell, Decadal trends in the North Atlantic oscillation: regional temperatures and precipitation, Science 296 (1995) 676–679.
[39] D. Kvasov, Paleohydrology of Eastern Europe in Late Quaternary time, Yezhegodnkkh Chetniyakh Pamyati L.S. Berga Doklady, Izd., Nauka, 1968, pp. 65–81.
[40] M.N. Cagatay, N. Görür, O. Algan, C. Eastoe, A. Tchepalyga, D. Ongan, T. Kuhn, I. Kuscu, Late Glacial–Holocene palaeoceanography of the Sea of Marmara: timing of connections with the Mediterranean and the Black Seas, Mar. Geol. 167 (2000) 191–206.
[41] M.A. Kaminski, A. Aksu, M. Box, R.N. Hiscott, S. Filipescu, M. Al-Salameen, Late Glacial to Holocene benthic foraminifera in the Marmara Sea: implications for Black Sea–Mediterranean Sea connections following the last deglaciation, Mar. Geol. 190 (2002) 165–202.
[42] G.A. Jones, A.R. Gagnon, Radiocarbon chronology of Black Sea sediments, Deep-Sea Res. I 41 (1994) 531–557.
[43] P.K. Swart, Factors influencing the oxygen isotopic composition of the Black Sea, in: E. Izdar, J.W. Murray (Eds.), Black Sea Oceanography, Kluwer Academic Publishers, Dordrecht, 1991, pp. 75–88.